International Symposium
On Turbulence and Shear Flow
Phenomena (TSFP-8)
August 28 - 30, 2013 Poitiers, France

INVESTIGATION OF THE LAW-OF-THE-WALL IN A TURBULENT BOUNDARY LAYER FLOW WITH ADVERSE PRESSURE GRADIENT AT $RE_\theta = 10000$ USING LARGE-SCALE PIV

Tobias Knopp, Daniel Schanz, Andreas Schröder
Institute of Aerodynamics and Flow Technology
German Aerospace Center (DLR)
Bunsenstr. 10, 37073 Göttingen, Germany
Tobias.Knopp@dlr.de, Daniel.Schanz@dlr.de, Andreas.Schroeder@dlr.de

Rainer Hain, Christian J. Kähler
Institute for Fluid Mechanics and Aerodynamics
Universität der Bundeswehr München (UniBw)
Werner-Heisenberg-Weg 39, 85577 Neubiberg, Germany
Rainer.Hain@unibw.de, Christian.Kaehler@unibw.de

ABSTRACT

We present an experimental investigation and data analysis of a turbulent boundary layer flow at a significant adverse pressure gradient at Reynolds number $Re_\theta = 10000$ using large field PIV. The aim is to find a wall-law for the mean-velocity in the inner layer. We consider scaling law diagnostic functions together with the Millikan argument. The inner part can be fitted by the log-law, but is progressively reduced. In the outer part, the overlap layer, the log-law ceases to be valid. Instead, a modified log-law gives a good fit, which needs as parameters the pressure gradient parameter and the mean inertial effects. We then attempt to find a quantitative description which is local in wall-normal direction without streamwise history effects.

INTRODUCTION

The statistically averaged behaviour of a turbulent boundary layer subjected to a significant adverse pressure gradient is still an open question. For a boundary layer at zero-pressure gradient, we assume that the log-law $u^+ = \log(y^+)/\kappa + B$ gives a proper description of the mean velocity at sufficiently large Reynolds numbers, see e.g. Österlund *et al.* (2000). There are different statements in the literature concerning the law-of-the-wall in adverse pressure gradient flows, see e.g. Alving & Fernholz (1995). The first hypothesis is the log-law still holds and that slope κ and intercept B still have the same value as for a flat-plate turbulent boundary layer at zero pressure gradient (ZPG) but that the region occupied by the log-law is progressively reduced. Some authors propose that beyond the log-law region there is a so-called half-power law region characterized by a shear stress growing linearly with the wall-distance, see e.g. Brown & Joubert (1969). The second hypothesis is that the log-law still holds but that κ and B change their values. Experimental results and DNS data give indications that κ and B could change, see Nickels (2004). Some publications propose a functional dependence on the so-called pressure gradient parameter $\Delta p_x^+ = \nu/(\rho u_\tau^3)\mathrm{d}p/\mathrm{d}x$, see Nickels (2004). The third hypothesis by (among others) Szablewski (1954), McDonald (1969) is that the pressure gradient causes a continuous, general breakdown of the log-law.

In order to shed some light on this question, by making use of the enormous progress of non-intrusive optical flow-field measurement techniques in the last years we designed a new flow experiment. Several requirements on the flow must be considered to prepare the desired flow features within the experiment. 1. The flow should start with a fully developed turbulent boundary layer at zero pressure gradient with established log-law region. 2. The Reynolds number needs to be sufficiently large such that a sufficiently thick log-layer forms, say $Re_\theta > 6000$ according to Österlund *et al.* (2000). 3. Downstream of this position of a well-defined inlet condition the flow enters into the adverse pressure gradient section. The flow development in streamwise direction should be slow, such that the successive changes in the log-law can be tracked and history effects can be avoided. 4. The pressure gradient needs to be sufficiently strong in order to cause changes from the universal law-of-the-wall, say $\Delta p_x^+ > 0.015$. 5. For the exact behaviour of the wall-law slope parameters, e.g. κ, a direct method for the wall-shear stress τ_w is needed. In this work, we use different indirect methods for τ_w which will be validated locally using a direct method later.

CLASSICAL THEORY

The turbulent boundary layer equations for the evolution of the wall-parallel mean velocity component U in incompressible flows without external forces can be written as

$$\nu\frac{\partial^2 U}{\partial y^2} - \frac{\partial \overline{u'v'}}{\partial y} = \frac{1}{\rho}\frac{\mathrm{d}P}{\mathrm{d}x} + U\frac{\partial U}{\partial x} + V\frac{\partial U}{\partial y} \qquad (1)$$

where we neglect $\nu\partial^2 U/x^2$ and $\partial\overline{u'u'}/\partial x$. Integration of (1) from the wall to y gives a relation for the total shear stress. We use viscous (inner) scaling coordinates $u^+ = U/u_\tau$, $y^+ = yu_\tau/\nu$, $\Delta p_x^+ = \nu/(\rho u_\tau^3)\mathrm{d}P/\mathrm{d}x$ and $I_{cu}^+(y^+) = I_{cu}u_\tau^{-2}$, $I_{cv}^+(y^+) = I_{cv}u_\tau^{-2}$ where we write the integrated convective (or: mean inertial) terms in the following form

$$I_{cu}(y) = \int_{y'=0}^{y} U\frac{\partial U}{\partial x}\mathrm{d}y' \ , \quad I_{cv}(y) = \int_{y'=0}^{y} V\frac{\partial U}{\partial y'}\mathrm{d}y' \ .$$

Then from (1) a relation for τ is obtained

$$\tau^+(y^+) \equiv \frac{\nu\frac{\partial U}{\partial y} - \overline{u'v'}}{u_\tau^2} = 1 + \Delta p_x^+ y^+ + I_{cu}^+(y^+) + I_{cv}^+(y^+) \ . \tag{2}$$

A scaling law $U(y)$ can be derived based on (2) together with the eddy-viscosity assumption and a mixing-length ansatz, see McDonald (1969), or by matching arguments between inner and outer scaling, cf. Millikan (1938), Gersten & Herwig (1992). Using the latter argument, the following diagnostic function should show a plateau in case that the underlying scaling law $U(y)$ is satisfied

$$\Xi = \frac{y^+}{\sqrt{\tau^+(y^+)}}\frac{\mathrm{d}u^+}{\mathrm{d}y^+} = \frac{1}{\kappa} \tag{3}$$

This argument involves τ, and using the present experimental data we will study whether the full form (2) or a linearized approximation for τ, e.g. by McDonald (1969)

$$\tau^+(y^+) \approx 1 + \lambda\Delta p_x^+ y^+ \tag{4}$$

is the proper choice within (3). McDonald (1969) approximates the effects of the convective term in (4) using $\lambda = 0.7$ for flows at mild pressure gradient near equilibrium. Integration of (2) yields, cf. e.g. Skote & Henningson (2002),

$$u^+ = \frac{1}{K_o}\log(y^+) + \frac{2}{K_o}\Big[\sqrt{1+\lambda\Delta p_x^+ y^+} - 1 + \log\left(\frac{2}{\sqrt{1+\lambda\Delta p_x^+ y^+}+1}\right)\Big] + B_o. \tag{5}$$

The theoretical mean velocity gradients corresponding to the log-law and (5) become $1/(\kappa y^+)$ and $\sqrt{1+\lambda\Delta p_x^+ y^+}/(K_o y^+)$.

A LOCAL MODEL FOR THE SHEAR STRESS

At this stage, the solutions for U and τ in (2), (4) and (5) are mutually coupled. The idea is now to use the linearized model (4) and to relate λ in (4) to the mean velocity profile by approximating the exact mean inertial terms. We follow van den Berg (1973) and assume that the velocity profile in the inner region can be described as $U(x,y) = u_\tau(x)f(y^+(x,y))$, $y^+(x,y) = u_\tau(x)y/\nu$, giving $\partial y^+/\partial y = u_\tau/\nu$ and $\partial y^+/\partial x = y/\nu\mathrm{d}u_\tau/\mathrm{d}x$. Then

$$\frac{\partial U}{\partial x} = \frac{\mathrm{d}u_\tau}{\mathrm{d}x}\left[f + y^+\frac{\mathrm{d}f}{\mathrm{d}y^+}\right] \ , \quad \frac{\partial U}{\partial y} = \frac{u_\tau^2}{\nu}\frac{\mathrm{d}f}{\mathrm{d}y^+}$$

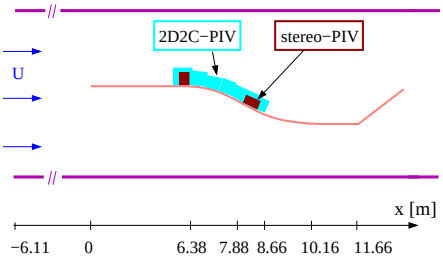

Figure 1. Sketch of the flow experiment and the PIV systems used (top view) at UniBw.

and V is obtained using the continuity equation. Substitution into (2) gives

$$\tau^+(y^+) = 1 + \alpha y^+ + \beta I_1 \tag{6}$$

with pressure gradient parameter α, wall shear stress gradient parameter β and I_1 defined by

$$\alpha \equiv \Delta p_x^+ = \frac{\nu}{\rho u_\tau^3}\frac{\mathrm{d}P}{\mathrm{d}x}, \quad \beta = \frac{\nu}{u_\tau^2}\frac{\mathrm{d}u_\tau}{\mathrm{d}x}, \quad I_1 = \int_0^{y^+} f^2\mathrm{d}y^+ \ .$$

This gives a model to relate the mean inertial terms to the streamwise gradient of the wall shear stress gradient.

As an extension, we assume that f becomes also a function of the pressure gradient parameter α, i.e., $U(x,y) = u_\tau(x)f(y^+(x,y),\alpha(x))$ leading to

$$\tau^+(y^+) \ = \ 1 \ + \ \alpha y^+ \ + \ \beta I_1 \ + \ \gamma I_2 \tag{7}$$

with an additional parameter $\gamma = -3\alpha\beta + \alpha^*$, $\alpha^* = \nu/u_\tau \times \nu/(\rho u_\tau^3)\ \mathrm{d}^2P/\mathrm{d}x^2$, where the role of $\mathrm{d}^2P/\mathrm{d}x^2$ is discussed e.g. in Hanjalic *et al.* (1999). Integral I_2 is given by

$$I_2 = 2\int_0^{y^+} f\ \frac{\partial f}{\partial\alpha}\ \mathrm{d}y^+ \ - \ f\int_0^{y^+}\ \frac{\partial f}{\partial\alpha}\ \mathrm{d}y^+ \ .$$

Here $\partial f/\partial\alpha$ may be evaluated e.g. by using a simple composite profile for f consisting of Chauhan *et al.* (2009) in the inner part of the inner layer and (5) in the outer part.

EXPERIMENTAL SETUP

The aim of this experiment was to enable PIV measurements in the inner part of the boundary layer by using relatively small onflow velocities and by making the Reynolds length and hence δ_{99} large. This also ensures a large Re_θ, i.e., a sufficiently large overlap layer, see Knopp (2011).

The experiments were performed in the Eiffel type atmospheric wind tunnel of the UniBw in Munich. The facility has a 22-m-long test section with a rectangular cross-section of $2\times 2\mathrm{m}^2$. The experiments were performed at three different onflow velocities, viz., $U_\infty = 6\mathrm{m/s}$, $U_\infty = 9\mathrm{m/s}$, and $U_\infty = 12\mathrm{m/s}$. The geometry is mounted vertically into the center of the tunnel, as shown in Fig. 1, see Dumitra *et al.* (2011) for details. Starting with a super-elliptic nose and a subsequent tripping from laminar to turbulent flow, the flow first develops over a flat plate of length 6m and reaches $Re_\theta = 8000$ for $U_\infty = 12\mathrm{m/s}$. Then the flow

enters into an adverse pressure gradient section via a deflection of length $l = 1.5$m and a subsequent inclined flat plate of length $l = 0.8$m at an opening angle of 13° with respect to the first flat plate. We reach $Re_\theta = 10000$ at $x = 7.38$m for $U_\infty = 12$m/s. The contour geometry was designed using the DLR TAU code, see Knopp (2011), using the Spalart-Allmaras and the SST k-ω RANS turbulence model to take into account the criteria explained in the introduction.

MEASURING TECHNIQUE

For the measurement technique, particle image velocimetry (PIV) was used for the mean velocity and for the Reynolds stresses determination. Eight PCO 4000 cameras with a resolution of 4008 × 2672 px each were used side by side and the mean velocity fields were calculated by averaging of up to 9000 independent velocity fields. This experimental arrangement using the lightsheets of two independent double pulse lasers enabled to measure instantaneous velocity fields with 2D2C-PIV from $x = 5.81$m to $x = 8.65$m, see Fig. 1. Moreover, stereo-PIV (2D3C-PIV) measurements were performed in two measurement windows at the end of the long flat plate and in the expansion region.

RESULTS AND ANALYSIS

In the present work we focus on the adverse pressure gradient region. The pressure gradient parameter Δp_x^+ along the contour is shown in Fig. 2. At present, u_τ is determined only indirectly using a standard and modified Clauser chart, as described in the next subsection. In order to validate the indirect method, we additionally performed measurements using long-range-microscope PIV (LR-PIV), but their postprocessing is not yet finished.

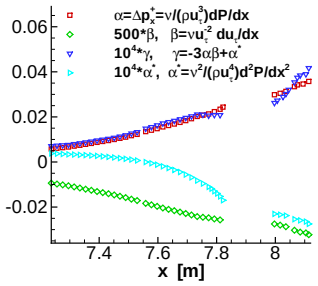

Figure 2. Characterization of the flow using pressure gradient parameter $\alpha \equiv \Delta p_x^+$, streamwise acceleration parameter β, $\alpha^* \sim \mathrm{d}^2P/\mathrm{x}^2$ and higher order parameter γ.

A COMPOSITE SCALING LAW FOR THE INNER LAYER

In the adverse pressure gradient region, the mean velocity profile can be described by a composite law as proposed by Brown & Joubert (1969) for $y^+ \gtrapprox 100$ and $y/\delta_{99} \lessapprox 0.2$. In its inner part, the velocity profile can by fitted by a log-law whereas in the outer part, an extended log-law (5) gives a suitable scaling, see Fig. 3 and Knopp *et al.* (2012).

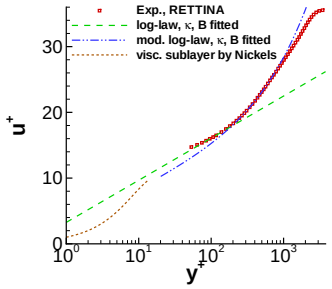

Figure 3. Composite structure of the mean velocity profile at $x = 7.61$m at adverse pressure gradient $\Delta p_x^+ = 0.0156$.

SCALING IN THE INNER PART OF THE INNER LAYER

In the inner part of the inner layer, we observe that the velocity profiles can be fitted using a log-law

$$u^+ = \frac{1}{K_\mathrm{i}} \log(y^+) + B_\mathrm{i} \tag{8}$$

in a thin region around $y^+ = 100$. This region will be called the log-law fit region. For the station $x = 7.73$m where $\Delta p_x^+ = 0.0202$ this region is located at $4.0\mathrm{mm} < y < 7.0\mathrm{mm} \approx 0.05\delta_{99.5}$ or $80 < y^+ < 140$, see Fig. 4. We determine u_τ using a standard and a modified Clauser chart method similar to the method by Dixit & Ramesh (2009), and we find that the values obtained for K_i are not very sensitive w.r.t. the method to determine u_τ. We observe a systematic reduction of K_i with increasing Δp_x^+ and that the correlation by Nickels (2004) gives a good quantitative description. Fig. 5 shows the data for the present experiment at $U_\infty = 12$m/s and for some data evaluated from literature. At this point, some words of caution are needed. The value for K_i given in Fig. 5 has to be seen as a fitting parameter for the inner part of the inner layer. It is not a general parameter for the entire overlap region as the von Kármán constant κ in zero-pressure gradient boundary layer flow. In the log-law fit region, we do not have a clear plateau in $\Xi_{\log} = y^+ \mathrm{d}u^+/\mathrm{d}y^+$, see Fig. 6. Thus the log-law fit is only an approximative description and K_i cannot be determined in a strict way. Furthermore the log-law fit region is rather thin and its outer limit cannot be extended by increasing *Re*

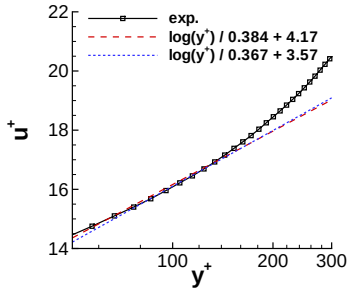

Figure 4. Log-law fit to the experimental data in the so-called log-law fit region around $y^+ = 100$ in the adverse pressure gradient region at $x = 7.73$m with $\Delta p_x^+ = 0.0202$.

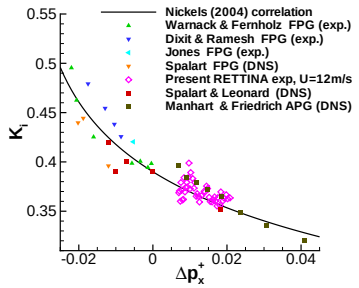

Figure 5. Variation of K_i vs. Δp_x^+ in the log-law fit region for the present experiment and for some data evaluated from literature.

like in the zero-pressure gradient case, since it is progressively reduced due to the adverse pressure gradient. Moreover it occupies a y^+-range, which is for zero-pressure gradient flows influenced by low-Re effects according to Wei *et al.* (2005*a*), Wei *et al.* (2005*b*) and Marusic *et al.* (2012). Albeit, we showed in Knopp *et al.* ((submitted) that the behaviour of this fit-K_i is relatively robust w.r.t. details how it is determined.

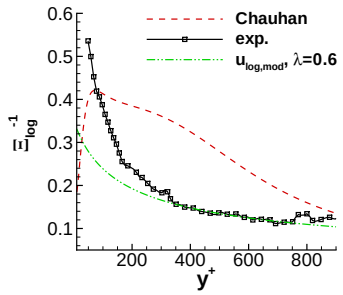

Figure 6. Diagnostic functions for the log-law applied to the experimental data in the adverse pressure gradient region at $x = 7.71$m with $\Delta p_x^+ = 0.0192$.

Mean momentum balance

The aim is now to undestand how the modified log-law (5) can give a reasonable description of the velocity gradient in the overlap layer, see Fig. 6. In the first step we want to identify the dominant terms of the mean momentum balance (1) which need to be taken into account into a simplified model (4). We consider the stereo-PIV data at $x = 8.07$m where $\Delta p_x^+ = 0.034$. The different terms of eq. (1) are shown in Figure 7. We see that the viscous stress gradient $-\nu\partial^2 U/\partial y^2$ and $\partial\overline{u'u'}/\partial x$ are much smaller than the pressure gradient and the mean inertial terms, albeit the viscous stress gradient cannot be resolved for $y^+ < 20$. The mean momentum balance is significantly altered due to the adverse pressure gradient compared to the zero pressure gradient case, see e.g. Wei *et al.* (2005*a*). Moreover we see that $V\partial U/\partial y$ is of the same size as $U\partial U/\partial x$ and that the mean inertial terms are of the same order of magnitude as the pressure gradient term. The Reynolds shear stress gradient $\partial\overline{u'v'}/\partial y$ can be reconstructed from the remaining terms in (1) and reaches its first zero at $y^+ \approx 500$ where $\overline{u'v'}$ has its first maximum.

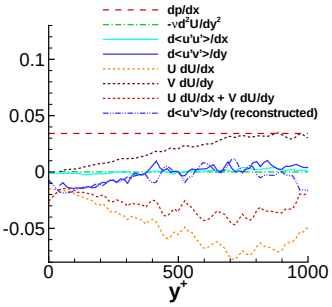

Figure 7. Order of magnitude analysis of the different terms in eq. (1) from the stereo-PIV data at $x = 8.07$m where $\Delta p_x^+ = 0.034$.

REYNOLDS SHEAR STRESS PROFILES

The second step is to find some approximative model for the shear stress $\tau^+(y^+)$. This is needed in order to assess the Millikan scaling law argument (3) and the linearized stress relation (4). We also compare $\tau = \nu \mathrm{d}U/\mathrm{d}y - \overline{u'v'}$ with different proposals to reconstruct τ, e.g., from the exact balance (2) or some approximation (6), (7).

The reconstructions based on the exact terms I_{cu} and I_{cv} are computed by numerical integration using the PIV data for U and V including the exact gradients $\partial U/\partial x$ and $\partial U/\partial y$. In the near wall region where the PIV data are not accurate enough, we use the profile by Chauhan *et al.* (2009). It becomes clear that I_{cv} cannot be neglected for $y^+ > 150$. The reconstructions based on the (6), (7) also use the PIV data for U and V in I_1 and in the near wall region we use the profile by Chauhan *et al.* (2009). For I_2 we use (5) with $\lambda = 0.4$ to estimate $\partial f/\partial\alpha$. Moreover we need to compute α, β and γ, which are shown in Fig. 2.

It can be seen from Fig. 8 that the estimate (6) is already a good approximation for the shear stress. The extended model (7) approximates the exact reconstruction (2) also for $y^+ \gtrapprox 300$. However, for $y^+ \gtrapprox 250$ we also observe some deviation between $\tau = \nu \mathrm{d}U/\mathrm{d}y - \overline{u'v'}$ and (2), which is not understood so far. We emphasize that both estimates (6) and (7) considerably improve the approximation of τ compared to the linear-stress relation $1 + \Delta p_x^+ y^+$ which neglects the effects of the mean inertial terms completely.

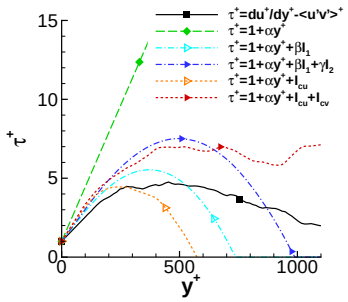

Figure 8. Comparison of $\tau = \nu \mathrm{d}U/\mathrm{d}y - \overline{u'v'}$ with different proposals for reconstruction using (2) and (6), (7) at $x = 8.08$m where $\Delta p_x^+ = 0.0344$.

SCALING IN THE OUTER PART OF THE OVERLAP LAYER

In the third step we consider the scaling law argument (3) which relates the gradient of the mean velocity profile, the wall distance and the shear stress τ, see Fig. 9. The aim is to find a proper choice for τ in (3). When using τ based on the exact profile of $\tau = \nu dU/dy - \overline{u'v'}$ and also based on the different reconstructions (2) and (6), (7), we do not obtain a plateau in Ξ. From this we infer that the exact $\tau^+(y^+)$ is not the suitable choice for τ in the scaling argument (3). On the other hand, the linearized model $\tau = 1 + \lambda \Delta p_x^+ y^+$ does give a plateau. This gives a motivation to assume a linearized stress relation (4) in the wall-law (5).

The fourth step is to identify the parameter λ in the linearized model $\tau = 1 + \lambda \Delta p_x^+ y^+$. It can be seen from Fig. 8 that τ^+ grows slower than $1 + \Delta p_x^+ y^+$ with increasing y^+ and also that the wall-normal stress gradient $\partial \tau^+ / \partial y^+$ decreases with increasing y^+ compared to Δp_x^+, see also Fig. 7. Hence a value of λ smaller than 1 is expected. Thus λ describes the effect of the mean inertial terms on the wall-normal shear stress gradient.

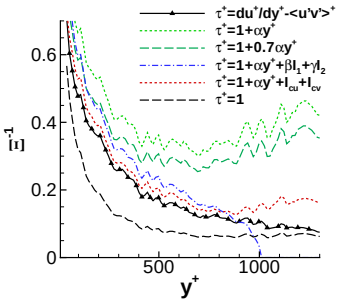

Figure 9. Comparison of slope diagnostic function Ξ with different proposals for τ in (3) using (2) and (6), (7) at $x = 8.07$m where $\Delta p_x^+ = 0.0342$.

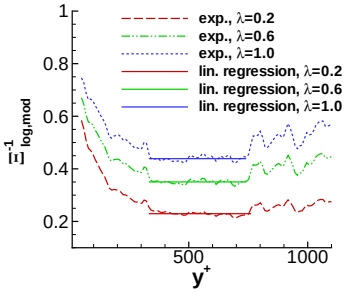

Figure 10. Diagnostic functions for the modified log-law, see Eq. (3), applied to the experimental data in the adverse pressure gradient region at $x = 7.71$m with $\Delta p_x^+ = 0.0192$.

Regarding the diagnostic function (3), the choice for λ in (4) effects the plateau value for K_0. Decreasing the value for λ gives a lower K_0 as shown in Fig. 10.

Now we focus on the wall-normal stress gradient $\partial \tau^+ / \partial y^+$. We write $\lambda \equiv (\partial \tau^+ / \partial y^+) / \Delta p_x^+$. At the position $x = 8.07$m direct data for $\overline{u'v'}$ are available. The exact reconstruction (2) and the approximation (6) give a quite good agreement whereas (7) is little larger. At $x = 7.75$m, data for $\overline{u'v'}$ are not available and we use (2) as a reference. The approximation (7) is given for two different values of λ and both choices are closer to (2) than (6) for $y^+ > 150$.

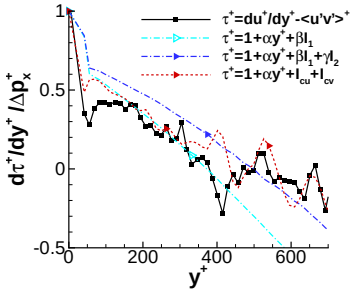

Figure 11. Comparison of $\partial \tau / \partial y$ with different reconstructions (2), (6), (7) at $x = 8.07$m where $\Delta p_x^+ = 0.0342$.

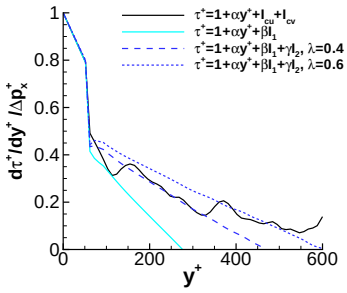

Figure 12. Comparison of different reconstructions (2), (6), (7) for $\partial \tau / \partial y$ at $x = 7.75$m where $\Delta p_x^+ = 0.0208$.

The last step is to assess the linearized shear stress model model $\tau = 1 + \lambda \Delta p_x^+ y^+$. We obtain a reasonable linear fit to the shear stress τ using $\lambda = 0.45$ found from Fig. 11 in the region between $y^+ = 100$ and $y^+ = 150$, as shown in Fig. 13. This linear approximation for τ is then used in the scaling law ansatz (3).

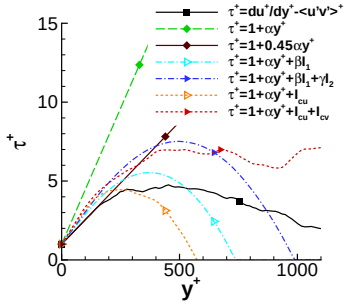

Figure 13. Comparison of $\tau = \nu dU/dy - \overline{u'v'}$ with linearized model (4) using $\lambda = 0.45$ obtained in the previous step at $y^+ \approx 150$ and different proposals for reconstruction using (2) and (6), (7) at $x = 8.08$m where $\Delta p_x^+ = 0.0344$.

We can use this linearized model for τ for a predictor-corrector type method for $u^+(y^+)$ in (5) and the parameter λ. Here we assume that α, β and γ are given.

1. Compute a first estimate for $\tau^+(y^+)$ using Eq. (6) with $u^+(y^+)$ given by the wall law of Chauhan *et al.* (2009)
2. Compute $\partial\tau^+/\partial y^+$ in the region $100 < y^+ < 200$ and set $\lambda = (\partial\tau^+/\partial y^+)/\Delta p_x^+$
3. Compute $u^+(y^+)$ in (5) with λ from step 2.
4. Compute an improved $\tau^+(y^+)$ using (7) and $u^+(y^+)$ from step 3.
5. Compute $\partial\tau^+/\partial y^+$ in the region $100 < y^+ < 200$ from step 4 and set $\lambda = (\partial\tau^+/\partial y^+)/\Delta p_x^+$
6. Compute $u^+(y^+)$ in (5) with λ from step 5.

CONCLUSION

We presented the analysis of experimental data of a turbulent boundary layer at a significant adverse pressure gradient using large-scale 2D2C-PIV and stereo-PIV. The mean velocity profiles in the inner layer can be described by a composite velocity profile similar to Brown & Joubert (1969). The inner part can be described as a "log-law fit" region with slope K_i changing w.r.t. Δp_x^+ as proposed by Nickels (2004). The outer part can be described by the modified log-law (5) by McDonald (1969), whose main parameters are the pressure gradient parameter Δp_x^+ and the shear-stress gradient parameter λ, which describes how the wall-normal shear stress gradient is influenced by the mean inertial terms. We extend the work by McDonald (1969) to account for the effect of the mean inertial terms on the shear stress gradient depending on the flow conditions instead of assuming it to be a constant fraction of Δp_x^+. For this purpose, we use and extend a simple model by van den Berg (1973) which is local in wall-normal direction and without streamwise history effects. This model enables a reasonable approximation for the wall-normal shear stress distribution and for the shear-stress gradient parameter λ.

For future work, we plan to validate the present model using the data for the two other onflow velocities, $U_\infty = 6\mathrm{m/s}$ and $U_\infty = 9\mathrm{m/s}$. Moreover, we plan to validate the indirect method for u_τ using directly measured data from LR-PIV in conjunction with a particle tracking velocimetry for post-processing, see Kähler *et al.* (2012).

ACKNOWLEDGEMENT

The authors are very grateful to Profs. Manhart and Warnack for providing their data.

REFERENCES

Alving, A. E. & Fernholz, H. H. 1995 Mean-velocity scaling in and around a mild, turbulent separation bubble. *Physics of Fluids* **7**, 1956–1969.

van den Berg, B. 1973 The law of the wall in two- and three-dimensional turbulent boundary layers. *Tech. Rep.*. NLR TR 72111 U.

Brown, K. C. & Joubert, P. N. 1969 The measurement of skin friction in turbulent boundary layers with adverse pressure gradients. *Journal of Fluid Mechanics* **35**, 737–757.

Chauhan, K. A., Monkewitz, P. A. & Nagib, H. M. 2009 Criteria for assessing experiments in zero pressure gradient boundary layers. *Fluid Dynamics Research* **41**, 021404.

Dixit, S. A. & Ramesh, O. N. 2009 Determination of skin friction in strong pressure-gradient equilibrium and near-equilibrium turbulent boundary layers. *Experiments in Fluids* **47**, 1045–1058.

Dumitra, M., Schanz, D., Schröder, A. & Kähler, C. J. 2011 Large-scale turbulent boundary layer investigation with multiple camera PIV and hybrid evaluation up to single pixel resolution. In *9th International Symposium on Particle Image Velocimetry, Kobe, Japan, July 21-23*.

Gersten, K. & Herwig, H. 1992 *Strömungsmechanik. Grundlagen der Impuls-, Wärme- und Stoffübertragung aus asymptotischer Sicht*. Vieweg.

Hanjalic, K., Hadzic, I. & Jakirlic, S. 1999 Modeling turbulent wall flows subjected to strong pressure variations. *Journal of Fluids Engineering – Transactions of the ASME* **121**, 57–64.

Kähler, C. J., Scharnowski, S. & Cierpka, C. 2012 On the uncertainty of digital PIV and PTV near walls. *Experiments in Fluids* **52**, 1641–1656.

Knopp, T. 2011 Entwurf eines Experimentes einer turbulenten Grenzschicht mit starkem Druckgradienten bei hohen Reynoldszahlen zur Entwicklung von Wandgesetzen bei Druckgradienten und zur Verbesserung von RANS Turbulenzmodellen. *Tech. Rep.*. DLR-IB 224-2011 C 106.

Knopp, T., Schanz, D., Schröder, A., Dumitra, M., Hain, R. & Kähler, C. J. (submitted) Experimental investigation of the log-law for an adverse pressure gradient turbulent boundary layer flow at Re_θ up to 10000. *Flow, Turbulence and Combustion* .

Knopp, T., Schanz, D., Schröder, A., Dumitra, M. & Kähler, C. J. 2012 Experimental investigation of the log-law for an adverse pressure gradient turbulent boundary layer flow at Re_θ up to 10000. In *Turbulence, Heat and Mass Transfer 7*.

Marusic, I., Monty, J. P., Hultmark, M. & Smits, A. J. 2012 On the logarithmic region in wall turbulence. *Journal of Fluid Mechanics* **716**, R3–1–R3–11.

McDonald, H. 1969 The effect of pressure gradient on the law of the wall in turbulent flow. *Journal of Fluid Mechanics* **35**, 311–336.

Millikan, C. B. 1938 A critical discussion of turbulent flows in channels and circular tubes. In *Proc. 5th Int. Congr. Applied Mechanics*, pp. 386–392. New York: Wiley.

Nickels, T. B. 2004 Inner scaling for wall-bounded flows subject to large pressure gradients. *Journal of Fluid Mechanics* **2004**, 217–239.

Österlund, J. M., Johansson, A. V., Nagib, H. M. & Hites, M. H. 2000 A note on the overlap region in turbulent boundary layers. *Physics of Fluids* **12**, 1–4.

Skote, A. & Henningson, D. S. 2002 Direct numerical simulation of a separated turbulent boundary layer. *Journal of Fluid Mechanics* **471**, 107–136.

Szablewski, W. 1954 Turbulente Strömungen in divergenten Kanälen. *Ingenieur-Archiv* **22**, 268–281.

Wei, T., Fife, P., Klewicki, J. & McMurtry, P. 2005*a* Properties of the mean momentum balance in turbulent boundary layer, pipe and channel flows. *Journal of Fluid Mechanics* **522**, 303–327.

Wei, T., Schmidt, R. & McMurtry, P. 2005*b* Comment on the clauser chart method for determining the friction velocity. *Experiments in Fluids* **38**, 695–699.